MATERIALS SCIENCE



# Design of flexible polyphenylene proton-conducting membrane for next-generation fuel cells

**Junpei Miyake,[1] Ryunosuke Taki,[1] Takashi Mochizuki,[1] Ryo Shimizu,[1] Ryo Akiyama,[2] Makoto Uchida,[2] Kenji Miyatake[1,2]***

**Proton exchange membrane fuel cells (PEMFCs) are promising devices for clean power generation in automotive, stationary, and portable applications. Perfluorosulfonic acid (PFSA) ionomers (for example, Nafion) have been the benchmark PEMs; however, several problems, including high gas permeability, low thermal stability, high production cost, and environmental incompatibility, limit the widespread dissemination of PEMFCs. It is believed that fluorine-free PEMs can potentially address all of these issues; however, none of these membranes have simultaneously met the criteria for both high performance (for example, proton conductivity) and durability (for example, mechanical and chemical stability). We present a polyphenylene-based PEM (SPP-QP) that fulfills the required properties for fuel cell applications. The newly designed PEM exhibits very high proton conductivity, excellent membrane flexibility, low gas permeability, and extremely high stability, with negligible degradation even under accelerated degradation conditions, which has never been achieved with existing fluorine-free PEMs. The polyphenylene PEM also exhibits reasonably high fuel cell performance, with excellent durability under practical conditions. This new PEM extends the limits of existing fluorine-free proton-conductive materials and will help to realize the next generation of PEMFCs via cost reduction as well as the performance improvement compared to the present PFSA-based PEMFC systems.**

## INTRODUCTION

Proton exchange membrane fuel cells (PEMFCs) produce electricity directly from hydrogen and oxygen and have been intensively developed as alternative energy–converting devices because of their intrinsic advantages, such as high efficiency and low pollution levels, which have enabled the recent commercialization of fuel cell vehicles. However, considerable efforts are still under way to further improve the performance, durability, and cost effectiveness of the PEMFC system (*1*, *2*).

Perfluorosulfonic acid (PFSA)–based ionomer (for example, Nafion) membranes have been mostly used as PEM components, because they show balanced properties in terms of proton conductivity and mechanical and chemical stability (*3*). However, the complicated synthetic process for PFSA ionomers has impeded diversification in molecular design, which limits the possibilities for further improvement of membrane properties. In contrast, fluorine-free, especially aromatic, ionomers have exceedingly high flexibility in molecular design, realized by various synthetic approaches (*4*–*8*). Many recent efforts have suggested that this class of ionomers is ripe for breakthroughs in performance: That is, fluorine-free aromatic ionomer membranes can have properties superior to those of PFSA ionomer membranes in terms of gas barrier properties; in thermal, mechanical, and chemical stability; and in proton conductivity, at lower cost (*9*–*14*). However, none of the existing fluorine-free aromatic ionomer membranes have all of these properties simultaneously.

Sulfonated polyphenylene (polyphenylene ionomer) is quite possibly the most promising candidate conceivable because of the absence of chemically vulnerable heteroatom linkages (for example, ether, sulfide, and sulfone groups) in the polymer main chain. Nevertheless, there have been few reports on polyphenylene ionomers because of their very limited synthetic approaches, low solvent solubility, insufficient membrane-forming capability, and poor mechanical strength (negligible bendability). Exceptional efforts have been undertaken to introduce flexible (that is, hairy-rod concept) or bulky side groups (*15*, *16*) and have demonstrated that some polyphenylene ionomer membranes exhibit excellent oxidative stability (*17*); however, none of these have simultaneously achieved sufficient membrane flexibility (for example, elongation at break > 50%) comparable to those of other common polymer membranes. Because these side groups often affect the polymer conformation and entanglement (for example, membrane-forming capability and flexibility), it has been unclear whether this drawback is an intrinsic limitation of polyphenylene ionomer membranes. Thus, development of novel design principles, instead of polymer side-chain chemistry, is an inevitable next step in attempting to implement polyphenylene ionomers as fuel cell membranes.

Many properties of polymers are determined by the stiffness of the polymer main chain or backbone. The backbone stiffness can be described by the persistence length ($l_p$), which is the characteristic length scale for the exponential decay of the backbone tangent-tangent correlation functions (*18*). Briefly, the $l_p$ describes the distance required for the backbone to bend by 90° on average (*19*). Thus, the $l_p$ of polymers with curved backbones is generally small. In addition, when the $l_p$ is much smaller than the contour length of the polymer (that is, sufficiently high degree of polymerization), the polymer behaves as a flexible coil. In the case of polyphenylene, the introduction of kinked *m*-phenylene groups (120°) into the backbone will lead to small $l_p$ values, and if the degree of polymerization is high enough, the kinked polyphenylene should behave like a flexible coil. This is desirable for polymer entanglement, which we reasoned would result in the formation of tough, flexible membranes. Some researchers have suggested that the introduction of the *m*-phenylene groups in other polymer structure systems [for example, carboxylated or sulfonated poly(arylene-*co*-arylene sulfone)s (*20*) and phosphonated poly(*m*-phenylene) (*21*)] might be advantageous for improving the membrane flexibility. However, to the best of our knowledge, there have been no reports of the use of *m*-phenylene groups in changing the $l_p$ value of polyphenylene backbones or the

[1]Clean Energy Research Center, University of Yamanashi, 4-4-37 Takeda, Kofu, Yamanashi 400-8510, Japan. [2]Fuel Cell Nanomaterials Center, University of Yamanashi, Kofu, Yamanashi 400-8510, Japan.
*Corresponding author. Email: miyatake@yamanashi.ac.jp

conformational behavior, aiming at practically flexible thin polyphenylene ionomer (that is, sulfonated polyphenylene) membranes.

Our investigation begins with the estimation of $l_p$ for polyphenylenes with various *p*- and *m*-phenylene ratios. Then, we propose a novel design principle, which is based on polymer main-chain chemistry ($l_p$), for flexible polyphenylene membranes. On the basis of this design principle, we demonstrate for the first time that a sulfonated polyphenylene (SPP-QP) can provide bendable, thin membranes that address all of the outstanding issues for fuel cell applications. We emphasize that our newly designed polyphenylene ionomer has a well-defined, defect-free structure, without any branches and/or solubilizing side groups. The SPP-QP ionomer consists of only three components: sulfonated *p*-phenylene and unsubstituted *p*- and *m*-phenylene groups. An optimally balanced combination of the *p*- and *m*-phenylene groups in the polymer backbone can provide unprecedented membrane flexibility, which has never been attainable for this class of ionomers. The chemical robustness of polyphenylene provides extremely high chemical stability, that is, SPP-QP membranes retain their initial excellent properties and performance even after accelerated oxidative degradation tests in Fenton's reagent as well as under practical fuel cell operating conditions.

## RESULTS

### A novel design principle for flexible polyphenylene membranes

Our novel design principle is outlined as follows (Fig. 1). (i) We estimate $l_p$ for polyphenylenes with several *p*- and *m*-phenylene ratios in the backbones. (ii) We select a polyphenylene structure whose $l_p$ is small enough (that is, flexible coil behavior). (iii) We design a novel monomer with the desired *p*-phenylene/*m*-phenylene ratio (determined above) and also with sufficiently larger molecular size in comparison with $l_p$. This design principle is based on the hypothesis that the coil-ensured monomer tends to take a flexible coil conformation even if copolymerization with other comonomers (in the present case, sulfonated phenylene) is performed.

The $l_p$ value is generally estimated from molecular dynamics simulations, which are computationally expensive. On the other hand, Zhang *et al.* (*18*) have recently demonstrated that $l_p$ can be predicted much more easily by numerically averaging backbone conformations over a set of suitably generated random dihedral angles, which only requires some basic molecular geometries (for example, backbone deflection angles) and the torsional potentials as inputs. We applied this technique to the polyphenylene structures, whose torsional potentials for biphenyl molecules were taken from the literature (*22*), in which the well-tested density functional theory Becke three-parameter Lee-Yang-Parr method, with a triple-ζ polarized basis set 6-311G(2d,p), was used. In all calculations, the backbone tangent-tangent correlation functions $\langle v_0 \cdot v_n \rangle$ for each oligomer were numerically averaged over 100,000 backbone conformations at 300 K. The calculation was performed with Mathematica (notebook can be found in the Supplementary Materials).

Figure 1A shows the calculated $l_p$ as a function of *m*-phenylene content. In the case of poly(*p*-phenylene), the calculated $l_p$ was infinity, because the modeled *p*-phenylene group (180°) provides a completely straight backbone. It has been reported that poly(*p*-phenylene) derivatives with bulky pendant side groups (for example, benzophenone) reduced $l_p$ to the order of tens of nanometers (note that this is still very large) (*23*); however, this approach is not applicable in the present case, because our target does not include polyphenylenes with bulky substituents. As expected, the introduction of the *m*-phenylene groups markedly reduced the linearity and calculated $l_p$ (Fig. 1A), that is, the $l_p$ values were infinity (0% *meta*), 2.67 nm (20% *meta*), 1.07 nm (50% *meta*), 0.66 nm (80% *meta*), and 0.54 nm (100% *meta*). The calculated $l_p$ values span a wide range, indicating that polyphenylenes can be stiff, semiflexible, or flexible, depending on the *p*- and *m*-phenylene ratios. The *m*-phenylene–rich polyphenylenes (*meta* ≥ 50%) were calculated to have sufficiently small $l_p$ values (≤1.1 nm), which are comparable to those of common flexible polymers, such as polyethylene ($l_p$, ca. 0.7 nm) (*19*). Although poly(*m*-phenylene) (100% *meta*) might be of interest due to its minimal $l_p$ (0.54 nm), we excluded this structure because of the low solvent solubility reported in the literature (*24*), probably due to its crystalline nature (*25*). Consequently, we selected a polyphenylene with 80% *m*-phenylene groups ($l_p$, 0.66 nm) and designed a novel QP monomer, according to our novel design principle (Fig. 1B). Note that the newly designed QP monomer contains the desired *m*-phenylene/*p*-phenylene ratio (*meta*/*para* = 4:1), as well as sufficiently larger molecular size (five phenylene groups) in comparison with $l_p$ (about two phenylene groups).

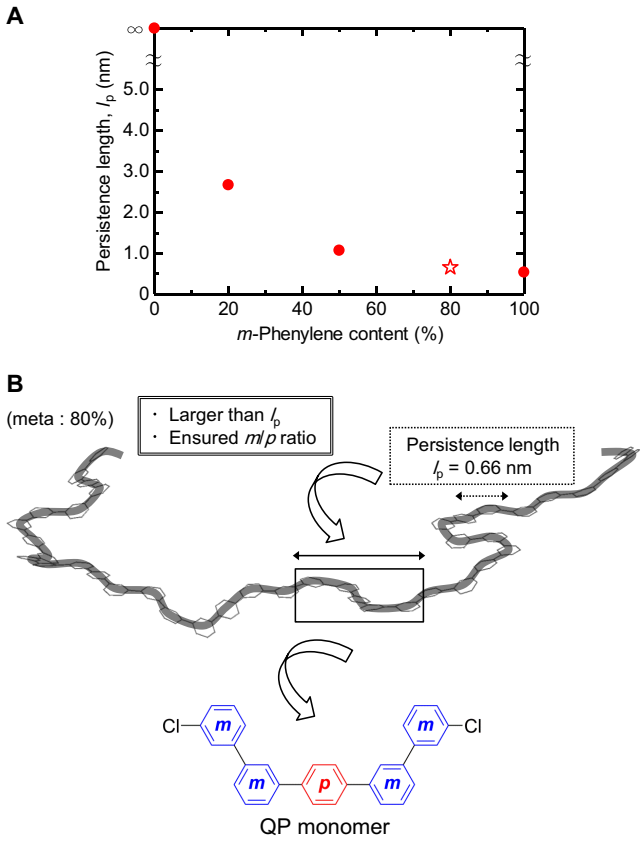


**Fig. 1. Novel design principle for flexible polyphenylene membranes.** (**A**) Estimated persistence length ($l_p$) of polyphenylenes. (**B**) Specific design of a novel monomer based on this principle.

### Polymer design and synthesis

The title sulfonated polyphenylene, SPP-QP, was synthesized from sulfonated phenylene (SP) and quinquephenylene (QP) monomers (Fig. 2A). The novel QP monomer, one *p*-phenylene capped with four *m*-phenylenes, was designed to enhance the polymer solubility and membrane flexibility, which was successfully synthesized by double

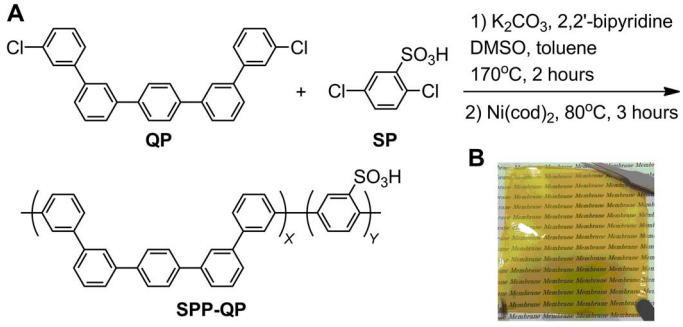


**Fig. 2. Novel polyphenylene-based PEM.** Synthesis (**A**) and membrane (**B**) of the SPP-QP.

Suzuki-Miyaura coupling reactions (figs. S1 to S3). The copolymerization reaction proceeded well via a Ni-mediated coupling reaction in a homogeneous system. The polyphenylene ionomers obtained were highly soluble in polar aprotic solvents, such as dimethyl sulfoxide (DMSO) and *N*,*N*′-dimethylformamide (DMF), but were not soluble in water or nonpolar organic solvents. The chemical structure of the SPP-QP copolymer was confirmed by $^1$H nuclear magnetic resonance (NMR) spectra (fig. S4), and the molecular weight was estimated from gel permeation chromatography (GPC) analysis to be $M_n = 7.7 \times 10^3$ and $M_w = 65 \times 10^3$. Casting from DMSO solution provided a thin, flexible, brown membrane (Fig. 2B). Among this class of ionomers (that is, sulfonated polyphenylenes), the membrane-forming capability of the SPP-QP ionomers was surprisingly high because of the well-balanced *p*-phenylene/*m*-phenylene ratio. The concentration of sulfonic acid groups or ion exchange capacity (IEC) of the SPP-QP membrane was estimated by acid base titration to be 2.4 mmol g$^{-1}$, which agrees with that (2.7 mmol g$^{-1}$) calculated from the $^1$H NMR spectrum.

As observed in the transmission electronic microscopy (TEM) image (fig. S5A), the SPP-QP (2.4 mmol g$^{-1}$) membrane (stained with $Pb^{2+}$ ions) exhibited a phase-separated morphology based on the hydrophilic-hydrophobic differences of its components. In the TEM image, the dark areas represent hydrophilic domains, and the bright areas represent hydrophobic domains. The domain sizes (ca. 3 nm in diameter for both domains) were uniform and much smaller than those of our reported aromatic block copolymer-based ionomer membranes (*12*), probably because of the random copolymer structure of the SPP-QP membrane.

Because the TEM image was necessarily obtained under dry conditions, further study needs to be conducted to obtain morphological information under practical conditions (for example, higher temperature with significant humidity). Thus, the morphology of the SPP-QP membrane was investigated with the small-angle x-ray scattering (SAXS) technique under both temperature- and humidity-controlled conditions [80°C and 30% relative humidity (RH)], and the scattered intensity as a function of the scattering vector (**q**) is shown in fig. S6. The SPP-QP membrane exhibited a single, clear peak at **q** = ca. 0.75 nm$^{-1}$ assignable to the ionic domains (*26*). The *d* spacing of the ionic domains was ca. 8.4 nm, which was somewhat higher than that observed in the TEM image (ca. 3 nm). The difference in the domain size would result from the difference in the IEC values (2.4 mmol g$^{-1}$ for TEM and 2.7 mmol g$^{-1}$ for SAXS) and the difference in the measurement environment (that is, temperature and humidity). Further investigation needs to be undertaken to understand the morphological behavior in more detail; however, we concluded that the SPP-QP membrane showed a well-defined phase-separated morphology.

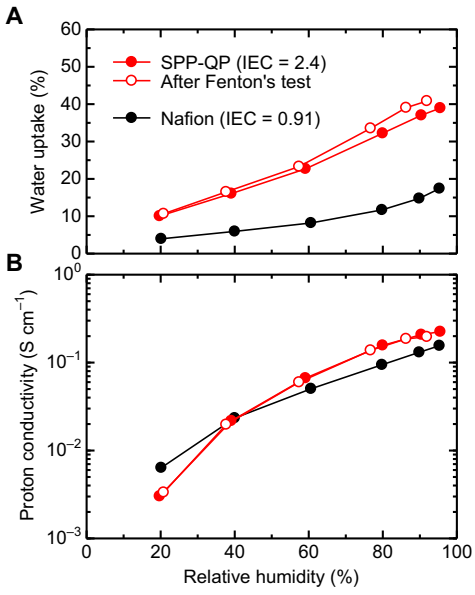


**Fig. 3. Water uptake and proton conductivity.** Humidity dependence at 80°C of (**A**) water uptake and (**B**) proton conductivity of PEMs. The IEC values (mmol g$^{-1}$) in parentheses were determined by acid base titration. Fenton's test was conducted by immersing the membrane in Fenton's solution (aqueous solution containing 3% $H_2O_2$ and 2 ppm $Fe^{2+}$) at 80°C for 1 hour. The solid lines are guides for the eye.

## Membrane properties

Figure 3 shows the water uptake and proton conductivity of PEMs at 80°C as a function of RH. The SPP-QP membrane was more hydrophilic, absorbing more water, than the Nafion membrane, because of the higher IEC of the SPP-QP membrane (2.4 mmol g$^{-1}$) compared with that of the Nafion membrane (0.91 mmol g$^{-1}$). The numbers of absorbed water molecules per sulfonic acid group (denoted as λ) for both PEMs were nearly comparable over a wide range of humidity (fig. S7). The SPP-QP membrane exhibits one of the highest proton conductivities among the reported fluorine-free aromatic ionomer membranes. The proton conductivity of the SPP-QP membrane (0.22 S cm$^{-1}$) was much higher than that of the Nafion membrane (0.16 S cm$^{-1}$) at 95% RH. The proton conductivity of these PEMs decreased with decreasing RH, and the SPP-QP membrane still had higher proton conductivity (22 mS cm$^{-1}$), comparable with that of the Nafion membrane, even under low humidity conditions (for example, 40% RH), owing to the well-developed, hydrophilic-hydrophobic, phase-separated morphology of the SPP-QP membrane (figs. S5A and S6). In addition, the conjugated structure of the polyphenylene main chain could contribute to the delocalization of negative charges; the sulfonic acid groups might dissociate more efficiently even under the relatively dry conditions, resulting in the high proton conductivity of the SPP-QP membrane.

The SPP-QP membrane also exhibited excellent mechanical stability under both dry and humidified conditions. Dynamic mechanical analysis (DMA) was conducted under similar conditions with those for the water uptake and proton conductivity measurements (Fig. 4). The viscoelastic properties of the SPP-QP membrane were not so sensitive to humidity (80°C, dry to wet) [that is, only a slight change in the storage modulus (*E*′) curve], and no transitions in the loss modulus (*E*″) and tan δ (= *E*″/*E*′) curves were observed. The SPP-QP membrane exhibited high *E*′ (>1 GPa) under the tested conditions, which exceeded that of the Nafion membrane by about one order of magnitude. This is

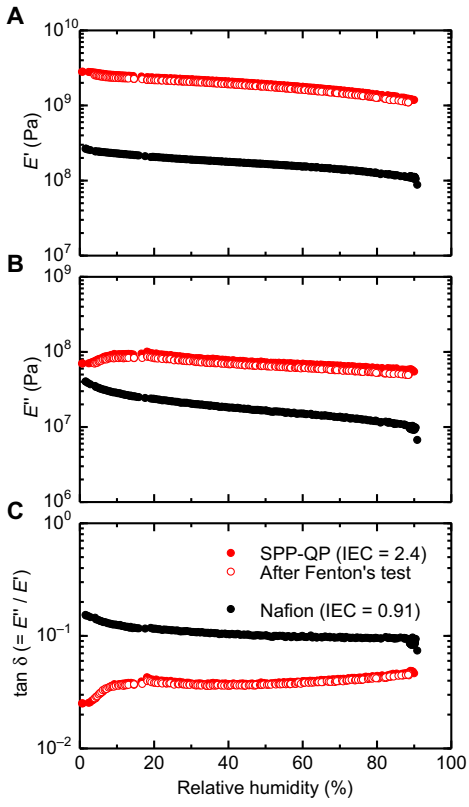


**Fig. 4. DMA analysis.** Humidity dependence at 80°C of (**A**) storage modulus ($E'$), (**B**) loss modulus ($E''$), and (**C**) tan δ (= $E''/E'$) of PEMs. Fenton's test was conducted by immersing the membrane in Fenton's solution (aqueous solution containing 3% $H_2O_2$ and 2 ppm $Fe^{2+}$) at 80°C for 1 hour.

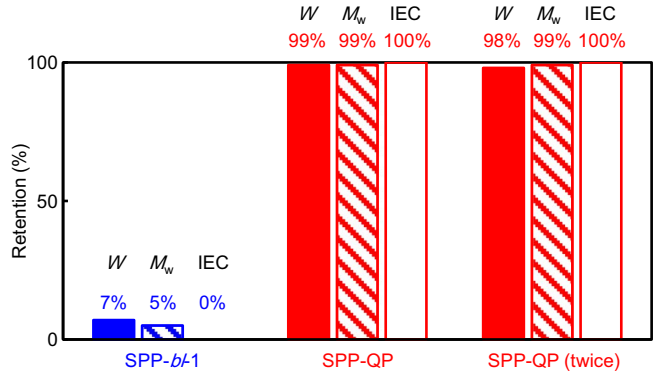


**Fig. 5. Oxidative stability test (Fenton's test).** Remaining weight ($W$), molecular weight ($M_w$), and IEC of the reference SPP-*bl*-1 (3.0 mmol $g^{-1}$) and SPP-QP (2.4 mmol $g^{-1}$) membranes after the Fenton's test (aqueous solution containing 3% $H_2O_2$ and 2 ppm $Fe^{2+}$, 80°C, 1 hour). The second Fenton's test of the first tested SPP-QP membrane was conducted, and the results are depicted as SPP-QP (twice). All IECs were determined by acid base titration. The chemical structure of the reference SPP-*bl*-1 copolymer is shown in fig. S9 (*27*).

surprising, considering the fact that the water uptake of the SPP-QP membrane was ca. 2.2 to 2.8 times higher than that of the Nafion membrane under the tested conditions (Fig. 3). The high mechanical stability of the SPP-QP membrane was further confirmed by a tensile test at 80°C (fig. S8). Under the humidified condition (60% RH), the SPP-QP membrane exhibited not only a reasonably high initial Young's modulus (1.3 GPa) and tensile strength (34 MPa) but also an unprecedentedly high elongation (strain at the break point = 68%) among the polyphenylene-based PEMs reported thus far. These values were comparable or higher than those of the reference SPP-*bl*-1 membrane (fig. S9) (*27*), which has the same sulfophenylene groups and rather flexible ether and sulfone linkages in the main chain; the initial Young's modulus, tensile strength, and strain at the break point of the reference SPP-*bl*-1 membrane with similar IEC value (2.7 mmol $g^{-1}$) were 1.1 GPa, 36 MPa, and 74%, respectively. More importantly, even under the reduced humidity conditions (20% RH), the SPP-QP membrane retained reasonably high elongation (strain at the break point = 39%), with a similar initial Young's modulus (1.1 GPa) and enhanced tensile strength (40 MPa). It has been believed that pure polyphenylenes yield brittle, nonductile membranes, which has hampered further development in the molecular design of this class of ionomers as PEMs. We emphasize here that the random coil structure (*28*), derived from the *m*-phenylene–rich polyphenylene backbone, as well as the absence of additional side chains and substituents, enhanced the interpolymer entanglement in the membrane and contributed to the marked improvement in membrane flexibility.

Hydrogen and oxygen gas permeabilities of the SPP-QP (2.4 mmol $g^{-1}$) and Nafion (0.91 mmol $g^{-1}$) membranes were measured at 80°C as a function of RH (fig. S10). The SPP-QP membrane exhibited significantly lower hydrogen and oxygen permeability over a wide range of humidity, from 30 to 90% RH. Although the gas permeability increased slightly with increasing humidity, the SPP-QP membrane still had superior gas barrier properties even under high humidity conditions; the hydrogen and oxygen permeabilities of the SPP-QP membrane were 20 and 15%, respectively, of those of the Nafion membrane at 90% RH. Similar superiority in gas barrier properties has been observed for aromatic copolymer-based ionomer membranes, including our own (*29*).

## Oxidative stability test (Fenton's test)

The SPP-QP membrane had unprecedentedly high oxidative stability. Figure 5 visualizes the result of the oxidative stability test in Fenton's reagent [aqueous solution containing 3% $H_2O_2$ and 2 parts per million (ppm) $Fe^{2+}$] at 80°C for 1 hour. It is well known that fluorine-free ionomer membranes degrade significantly under these harsh conditions via the oxidative attack by hydroxyl radicals. The reference SPP-*bl*-1 membrane (fig. S9) (*27*) containing heteroatom linkages (for example, ether, sulfone, and ketone groups) in the main chain broke into pieces; the remaining weight (7%), molecular weight (5%), and IEC (0%) of the SPP-*bl*-1 membrane were seriously affected. By contrast, the SPP-QP membrane was much more stable, with nearly perfect retention of properties: remaining weight (99%), molecular weight (99%), and IEC (100%). The nearly perfect retention of the properties was still observed even after repeating the test twice (that is, 2 hours in total): remaining weight (98%), molecular weight (99%), and IEC (100%). Surprisingly, the SPP-QP membrane also retained its flexibility, without cracks or brittleness (fig. S11). These results are unusual (*17*); most aromatic ionomer membranes exhibit much more severe chemical degradation and/or severe physical changes, including cracking, fracturing, or dissolution, in hot Fenton's reagent. The extremely high chemomechanical stability of the SPP-QP membrane is most likely to be based on the molecular design, that is, the chemical robustness of the polyphenylene main chain without heteroatom groups contributes to the retention of the molecular structure and also the retention of the interpolymer entanglement in the membrane.

The extremely high chemomechanical stability of the SPP-QP membrane made it possible to further examine the wide varieties of posttest analysis of the membrane. First, $^1$H NMR spectra were identical before and after the Fenton's test (fig. S4), indicating that the chemical structure was negligibly affected either in the polyphenylene backbone or in the attached sulfonic acid groups. Unlike the existing fluorine-free ionomers containing similar sulfophenylene units, the sulfonic acid groups were intact in the SPP-QP membrane, possibly because the conjugated structure of the polyphenylene main chain was able to delocalize the negative charges of the sulfonate groups, resulting in the stabilization of the phenylene-$SO_3^-$ bonding under the oxidative conditions. In addition, the phase-separated morphology of the SPP-QP membrane was also identical before and after the Fenton's test (fig. S5B). Surprisingly, the Fenton's test had little effect on the membrane properties: The proton conductivity (Fig. 3B) and the viscoelastic properties (Fig. 4) of the SPP-QP membrane were retained perfectly. A slight increase in water uptake (Fig. 3A) and a slight decrease in mechanical strength (fig. S8) were observed, indicating that the Fenton's test might have caused slight changes in the polymer interactions and/or entanglement inside the membrane. Accordingly, it is suggested that not only the high chemical stability of the components (that is, sulfonated polyphenylenes) but also the optimal polymer interactions and/or entanglement (that is, random coil structure) are crucial points in enhancing the membrane stability in hot Fenton's reagent.

## Fuel-cell performance and durability

A membrane electrode assembly (MEA) was fabricated with an SPP-QP membrane and subjected to fuel cell performance tests at 80°C. It should be noted that Nafion was used as a binder in the catalyst layer (CL), because these PFSA-based ionomers are still the state-of-the-art materials and are well tested as binder materials. Figure 6 (A and B) shows polarization curves [ohmic (*IR*) drop–included] and ohmic resistances under humidity conditions of 100 and 30% RH. At 100% RH (Fig. 6A), the open circuit voltage (OCV) of the cell was 1.04 V, indicating the good gas barrier properties of the SPP-QP membrane. Furthermore, the cell showed reasonably low ohmic resistance (ca. 0.06 ohm·cm$^2$) because of its high proton conductivity under the fully humidified conditions. The ohmic resistance at 30% RH (Fig. 6B) was larger due to the decreased proton conductivity of the SPP-QP membrane, but decreased with increasing current density, because the product water humidified the membrane. Therefore, the ohmic resistance (ca. 0.15 ohm·cm$^2$ at >0.6 A·cm$^{-2}$) agreed with that (0.15 ohm·cm$^2$) calculated from its proton conductivity at a slightly higher RH (ca. 40% RH) than that at 30% RH. Because of its high proton conductivity and good compatibility with the CLs, the SPP-QP cell exhibited high fuel cell performance even under low humidity conditions.

We then conducted an OCV hold test at 80°C and 30% RH (Fig. 6C). Under these conditions, the membrane degradation is accelerated because of the increased formation of hydrogen peroxide and the resulting formation of highly oxidizing radical species (*30*). As reported by many researchers, we have also demonstrated that the OCV of a Nafion-based cell dropped after only 140 hours (*31*). In contrast, the change in the OCV of the SPP-QP cell (ca. 226 μV hour$^{-1}$) was much slower than that of the Nafion cell under the same conditions; the SPP-QP cell retained a high OCV even after 1000 hours. The ohmic resistance of the cell did not change. Posttest analysis revealed that changes in the molecular structure ($^1$H NMR spectra) and the molecular weight (GPC profiles) of the SPP-QP membrane were minor even after conducting an OCV hold test for 1000 hours (fig. S12). The extraordinarily high oxidative

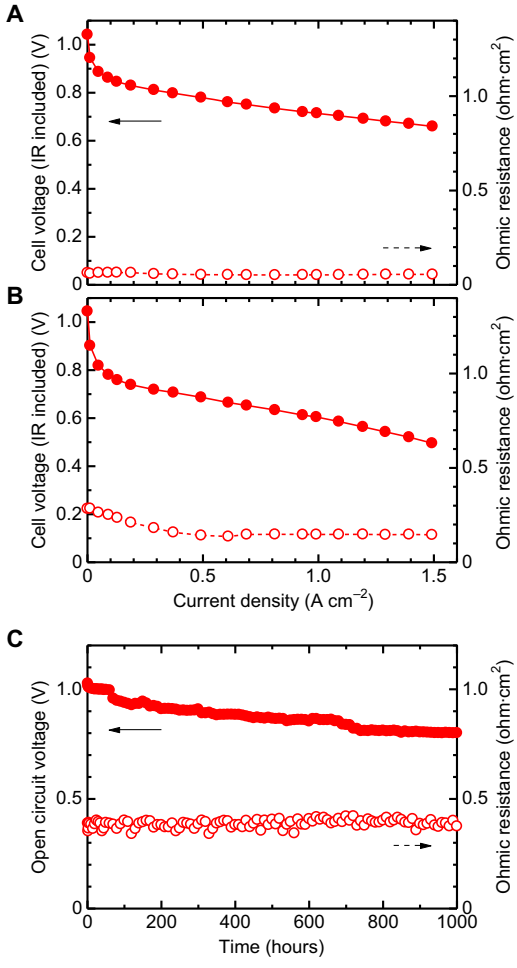


**Fig. 6. Fuel cell performance and durability (OCV hold test).** *IR*-included $H_2/O_2$ polarization curves (solid symbols) and ohmic resistances (open symbols) of the SPP-QP cell (IEC = 2.6 mmol g$^{-1}$) at 80°C under humidity conditions of (**A**) 100% RH and (**B**) 30% RH. (**C**) Changes in the cell voltage (solid symbols) and ohmic resistance (open symbols) of the SPP-QP cell (IEC = 2.6 mmol g$^{-1}$) at 80°C and 30% RH ($H_2$/air).

stability of the SPP-QP cell is likely to be due to the chemically robust nature as well as the low gas permeability of the SPP-QP membrane.

Under practical fuel cell operating conditions, mechanical durability involving wet-dry cycling is also a key issue. It has been reported that hydrocarbon ionomer membranes exhibited lower wet-dry cycle durability than those for PFSA membranes (*32*), mainly due to the lower dimensional stability (or higher water absorbability) of hydrocarbon ionomer membranes. Thus, the wet-dry cycle durability of the SPP-QP membrane was evaluated by means of the U.S. Department of Energy (DOE) protocol (*33*, *34*). As a preliminary result, the SPP-QP membrane lasted more than 6000 wet-dry cycles without mechanical failure (without increase in gas permeability). To the best of our knowledge, this is the first example of a polyphenylene ionomer membrane exhibiting such high wet-dry cycle durability, which might be due to the high flexibility in this class of ionomer membrane (that is, polyphenylene). Continuation of the wet-dry cycling test (for example, up to 30,000 wet-dry cycles) and other stability evaluations under much harsher conditions (for example, OCV hold test combined with wet-dry cycling) are in our future agenda and will be reported elsewhere.

## DISCUSSION

We have successfully designed and synthesized a novel fluorine-free aromatic ionomer (SPP-QP) composed of only three components: sulfonated *p*-phenylene (SP) and unsubstituted *p*- and *m*-phenylene (QP). The simplest polymer structure would be advantageous from cost and scalability perspectives; that is, the hydrophilic (SP) monomer is commercially available, and the novel hydrophobic (QP) monomer is easily synthesized in only two steps from commercially available reagents, without any time-consuming purification processes (for example, silica gel column chromatography). The well-balanced combination of *p*- and *m*-phenylene in the polyphenylene backbone provided unexpectedly high membrane flexibility within this class of ionomers (that is, sulfonated polyphenylenes). The separated hydrophilic (SP) and hydrophobic (QP) segments in the polymer structure contributed to the high proton conductivity and fuel cell performance even under low humidity conditions. The SPP-QP membrane exhibited extraordinarily high oxidative stability, that is, the SPP-QP membrane retained its molecular structure and initial excellent properties (for example, proton conductivity, mechanical stability, and fuel cell performance) even after accelerated oxidative degradation tests under both Fenton's test conditions and operando fuel cell (OCV hold test) conditions. This chemical stability, together with sufficient membrane flexibility (for example, elongation at break > 50%), is, to the best of our knowledge, unprecedented among fluorine-free aromatic ionomer membranes. The high chemical stability of the components (that is, sulfonated polyphenylenes without heteroatom linkages in the main chain) as well as the optimal polymer interactions and/or entanglement (that is, random coil structure) are proposed to have enhanced the SPP-QP membrane characteristics, both chemically and physically; these may be important clues to further extend the superiority of fluorine-free aromatic ionomer membranes.

## MATERIALS AND METHODS

### Chemicals

1,4-Phenylenediboronic acid (TCI), 1-bromo-3-iodobenzene (TCI), tri(*o*-tolyl)phosphine [P(*o*-tol)$_3$] (TCI), palladium acetate [Pd(OAc)$_2$] (TCI), 3-chlorophenylboronic acid (Kanto Chemical), 2,5-dichlorobenzenesulfonic acid dihydrate (SP monomer) (TCI), 2,2′-bipyridine (TCI), and bis(1,5-cyclooctadiene)nickel(0) [Ni(cod)$_2$] (Kanto Chemical) were used as received. Other chemicals were of commercially available grade and used as received. According to the literature (*27*), the reference copolymer SPP-*bl*-1 ($M_n$ = 31 × 10$^3$ and $M_w$ = 172 × 10$^3$) was synthesized from the SP monomer and the chlorine-terminated oligo(arylene ether sulfone ketone) ($n$ = 4.9) via a Ni-mediated coupling reaction.

### Synthesis of QP monomer

The QP monomer was synthesized in two steps from commercially available reagents. The first step is the synthesis of 3,3″-dibromo-*para*-terphenyl. A 1-liter one-neck round-bottomed flask equipped with a condenser, a nitrogen purge, and a magnetic stirring bar was charged with 1,4-phenylenediboronic acid (9.76 g, 58.9 mmol), 1-bromo-3-iodobenzene (50.0 g, 177 mmol), P(*o*-tol)$_3$ (1.34 g, 4.42 mmol), 2 M aqueous $K_2CO_3$ (100 ml, 200 mmol), toluene (320 ml), and ethanol (120 ml). Palladium acetate (198 mg, 0.883 mmol) was added to this suspension. The mixture was stirred at 80°C for 18 hours, cooled to room temperature, and diluted with deionized water and toluene. Insoluble material was removed by filtration through a Celite plug. After separation of two layers, the aqueous layer was extracted with toluene, and the combined organic layers were concentrated in vacuo. Methanol was added to the residue, and the mixture was sonicated. The resulting solid was filtered, washed with methanol, and dried at 60°C under reduced pressure to afford 3,3″-dibromo-*para*-terphenyl as a light yellow solid (15.6 g, 68% yield). Then, the targeted QP monomer was synthesized. A 500-ml one-neck round-bottomed flask equipped with a condenser, a nitrogen purge, and a magnetic stirring bar was charged with 3-chlorophenylboronic acid (25.2 g, 161 mmol), 3,3″-dibromo-*para*-terphenyl (15.6 g, 40.2 mmol), sodium carbonate (17.1 g, 161 mmol), DMF (120 ml), and deionized water (160 ml). Palladium acetate (903 mg, 4.02 mmol) was added to this suspension. After stirring at 60°C for 24 hours, the reaction mixture was cooled to room temperature and diluted with deionized water and toluene. Insoluble material was removed by filtration through a Celite plug. The filtrate was washed with deionized water and concentrated in vacuo. Methanol was added to the residue, and the mixture was sonicated. The resulting gray solid was filtered, washed with methanol, and purified by treating with activated carbon (ca. 2 g) in ethyl acetate/dichloromethane (1:2, ca. 700 ml). Finally, the desired QP monomer was obtained as a white solid (14.2 g, 78% yield).

### Synthesis of SPP-QP copolymer

A typical procedure is as follows (titrated IEC = 2.4 mmol g$^{-1}$). A 100-ml three-neck flask equipped with a magnetic stirring bar and a nitrogen inlet/outlet was charged with SP monomer (0.664 g, 2.52 mmol), QP monomer (0.500 g, 1.10 mmol), $K_2CO_3$ (0.384 g, 2.78 mmol), 2,2′-bipyridine (1.78 g, 11.4 mmol), DMSO (22 ml), and toluene (4 ml). After the dehydration process at 170°C for 2 hours with a Dean-Stark trap, the reaction mixture was cooled to 80°C followed by the addition of Ni(cod)$_2$ (3.00 g, 10.9 mmol). After the reaction at 80°C for 3 hours, the reaction mixture was poured into methanol. The crude product was washed with 6 M hydrochloric acid and deionized water several times. Drying in a vacuum oven at 80°C yielded the targeted copolymer (97% yield).

### Membrane preparation

The SPP-QP copolymer was dissolved in DMSO and cast onto a flat glass plate. Drying the solvent yielded a thin (for example, 30 μm thickness), transparent, flexible, and brown membrane. The obtained membrane was treated with 1 M sulfuric acid, washed with deionized water several times, and dried at room temperature.

### Spectroscopy

$^1$H (500 MHz) and $^{13}$C (125 MHz) NMR spectra were obtained with a JEOL JNM-ECA 500 spectrometer using $CDCl_3$ or DMSO-$d_6$ as a solvent and tetramethylsilane as an internal reference.

### Molecular weight analysis

The apparent molecular weight was estimated from GPC measurement (eluent, DMF containing 0.01 M LiBr; column, Shodex K-805L; detector, Jasco 805 UV) at 50°C. Molecular weight was calibrated with standard polystyrene samples.

### Titration

The IEC of the membrane was determined by acid base titration. A piece of the membrane (ca. 20 mg) was equilibrated in an aqueous 2 M NaCl solution for 24 hours at room temperature. The released HCl by the ion exchange reaction was titrated with a standard 0.01 M aqueous NaOH solution at room temperature.

### Morphology

For the TEM observation, the membrane samples were stained in a 0.5 M $Pb(OAc)_2$ aqueous solution, embedded in epoxy resin, sectioned to 50 nm thickness, and placed on copper grids. Images were obtained using a Hitachi H-9500 microscope with an accelerating voltage of 200 kV. The SAXS experiment was conducted using a Rigaku NANO-Viewer diffractometer equipped with a temperature/humidity-controlled chamber. The membrane was equilibrated for at least 2 hours under the tested condition (that is, 80°C and 30% RH). Details on the measurement were described in our previous paper (*26*).

### Water uptake and proton conductivity

Water uptake and in-plane proton conductivity of the PEMs were measured simultaneously at 80°C with a solid electrolyte analyzer system (MSBAD-V-FC, Bel Japan Co.) in a temperature- and humidity-controllable chamber. The weight was measured by a magnetic suspension balance. Vacuum drying for 3 hours at 80°C provided the dry weight, and exposure to the given humidity for at least 2 hours provided the wet weight. The water uptake (%) was calculated from the following equation: (wet weight − dry weight)/dry weight × 100. The in-plane proton conductivity was measured using a four-probe conductivity cell equipped with an ac impedance analyzer (Solartron 1255B and 1287, Solartron Inc.). Ion-conducting resistance [$R$ (ohm)] was determined by the impedance plot obtained in the frequency range of 1 to $10^5$ Hz. The proton conductivity ($\sigma$) was calculated from the following equation: $\sigma = l/(A \times R)$, where $l$ (cm) and $A$ ($cm^2$) are the distance between the two reference electrodes and the cross-sectional area, respectively.

### Mechanical properties

DMA of the PEMs (5 × 30 mm) was carried out with an ITK DVA-225 dynamic viscoelastic analyzer. The humidity dependence of the storage modulus [$E'$ (Pa)], loss modulus [$E''$ (Pa)], and tan $\delta$ (= $E''/E'$) at 80°C was investigated at a humidification rate of 1% RH $min^{-1}$. A tensile test of the PEMs [DIN-53504-S3, dumbbell shape of 35 × 6 mm (total) and 12 × 2 mm (test area)] was conducted with a Shimadzu AGS-J 500N universal test machine equipped with a temperature- and humidity-controllable chamber. After equilibrating the sample for at least 3 hours under the tested conditions (that is, 80°C and 60 or 20% RH), the stress-strain curve was obtained at a stretching rate of 10 mm $min^{-1}$.

### Gas permeability

Hydrogen and oxygen permeability was measured using a GTR-Tech 20XFYC gas permeation measurement apparatus. The concentrations of the permeated gases were quantified using a Yanaco G2700T gas chromatograph with a Porapak Q column and a thermal conductivity detector. Argon and helium were used as the carrier gases for the measurement of hydrogen and oxygen, respectively. Membranes were placed in the center of the cells having gas inlet/outlets on both sides of the membranes. The test gas was supplied on one side of the membrane, and the carrier gas was supplied on the other side of the membrane. The same humidity conditions were applied to both test and carrier gases to ensure homogeneous wetting of the membranes. The membrane was equilibrated until stable permeation data were obtained. The gas permeation coefficient, $Q$ [$cm^3$ (STD) cm $cm^{-2}$ $s^{-1}$ $cmHg^{-1}$], was calculated by the following equation: $Q = 273/T \times 1/A \times B \times 1/t \times l \times 1/(76 - P_{H2O})$, where $T$ (K) is the absolute temperature, $A$ ($cm^2$) is the permeation area, $B$ ($cm^3$) is the volume of permeated test gas, $t$ (s) is the sampling time, $l$ (cm) is the thickness of the membrane, and $P_{H2O}$ (cmHg) is the water vapor pressure.

### Oxidative stability test (Fenton's test)

Iron(II) sulfate heptahydrate ($FeSO_4$ $7H_2O$) was used as an $Fe^{2+}$ source. Oxidative stability was tested by immersing the PEMs ($H^+$ form) in Fenton's reagent (aqueous solution containing 3% $H_2O_2$ and 2 ppm $Fe^{2+}$) at 80°C for 1 hour. Posttest analysis of the PEMs was conducted in terms of weight, molecular weight, IEC (titration), molecular structure ($^1$H NMR), water uptake, proton conductivity, and mechanical properties (DMA and tensile test).

### MEA fabrication

A catalyst paste was prepared by mixing commercial Pt/CB (carbon black) catalyst (TEC10E50E, Tanaka Kikinzoku Kogyo K.K.), Nafion dispersion (IEC = 0.95 to 1.03 mmol $g^{-1}$; D521, DuPont), deionized water, and ethanol by ball milling for 30 min. The mass ratio of Nafion binder to the carbon support (N/C) was adjusted to 0.70. The catalyst-coated membranes (CCMs) were prepared by spraying the catalyst paste on both sides of the membranes by means of the pulse-swirl-spray technique. The CCMs were dried at 60°C for 12 hours and hot-pressed at 140°C and 10 kgf $cm^{-2}$ for 3 min. The geometric area and the Pt-loading amount of the CL were 4.41 $cm^2$ and 0.50 ± 0.02 mg $cm^{-2}$, respectively. The CCMs were sandwiched between two gas diffusion layers (GDL, 29BC, SGL Group Co. Ltd.) and mounted into a cell, which had serpentine flow channels on both the anode and the cathode carbon separators.

### Fuel cell performance and durability

To evaluate the cell performance, polarization curves were measured at 80°C and 30 and 100% RH. Pure hydrogen and oxygen were supplied to the anode and the cathode, respectively. The gas utilizations at the anode and the cathode were 70 and 40%, respectively. The high-frequency resistance of the cell was measured with an ac milliohmmeter (model 3356, Tsuruga Electric Corporation) at 1.0 kHz. The OCV hold test was conducted at 80°C and 30% RH for 1000 hours. The flow rate of both pure hydrogen and air was 100 ml $min^{-1}$. The wet-dry cycle durability was evaluated by the DOE protocol. Details on the evaluation conditions were described in our previous paper (*34*).

## SUPPLEMENTARY MATERIALS

Supplementary material for this article is available at http://advances.sciencemag.org/cgi/content/full/3/10/eaao0476/DC1

fig. S1. Synthesis of QP monomer.
fig. S2. NMR assignment of 3,3″-dibromo-*para*-terphenyl.
fig. S3. NMR assignment of QP monomer.
fig. S4. $^1$H NMR assignment of SPP-QP (titrated IEC = 2.4 mmol $g^{-1}$) copolymer.
fig. S5. Morphology of SPP-QP (titrated IEC = 2.4 mmol $g^{-1}$) membrane.
fig. S6. SAXS profile.
fig. S7. Number of absorbed water molecules per sulfonic acid group ($\lambda$).
fig. S8. Stress versus strain curves.
fig. S9. Chemical structure of the SPP-*bl*-1 copolymer.
fig. S10. Hydrogen and oxygen permeability.
fig. S11. Membrane durability and flexibility.
fig. S12. The effect of the OCV hold test on the molecular structure of the SPP-QP membrane (IEC = 2.6 mmol $g^{-1}$).
Mathematica Notebook

## REFERENCES AND NOTES

1. C. H. Park, S. Y. Lee, D. S. Hwang, D. W. Shin, D. H. Cho, K. H. Lee, T.-W. Kim, T.-W. Kim, M. Lee, D.-S. Kim, C. M. Doherty, A. W. Thornton, A. J. Hill, M. D. Guiver, Y. M. Lee, Nanocrack-regulated self-humidifying membranes. *Nature* **532**, 480–483 (2016).
2. K.-S. Lee, J. S. Spendelow, Y.-K. Choe, C. Fujimoto, Y. S. Kim, An operationally flexible fuel cell based on quaternary ammonium-biphosphate ion pairs. *Nat. Energy* **1**, 16120 (2016).

3. K. A. Mauritz, R. B. Moore, State of understanding of Nafion. *Chem. Rev.* **104**, 4535–4586 (2004).
4. M. A. Hickner, H. Ghassemi, Y. S. Kim, B. R. Einsla, J. E. McGrath, Alternative polymer systems for proton exchange membranes (PEMs). *Chem. Rev.* **104**, 4587–4612 (2004).
5. T. J. Peckham, S. Holdcroft, Structure-morphology-property relationships of non-perfluorinated proton-conducting membranes. *Adv. Mater.* **22**, 4667–4690 (2010).
6. C. H. Park, C. H. Lee, M. D. Guiver, Y. M. Lee, Sulfonated hydrocarbon membranes for medium-temperature and low-humidity proton exchange membrane fuel cells (PEMFCs). *Prog. Polym. Sci.* **36**, 1443–1498 (2011).
7. H. Zhang, P. K. Shen, Recent development of polymer electrolyte membranes for fuel cells. *Chem. Rev.* **112**, 2780–2832 (2012).
8. K.-D. Kreuer, Ion conducting membranes for fuel cells and other electrochemical devices. *Chem. Mater.* **26**, 361–380 (2014).
9. N. Asano, M. Aoki, S. Suzuki, K. Miyatake, H. Uchida, M. Watanabe, Aliphatic/aromatic polyimide ionomers as a proton conductive membrane for fuel cell applications. *J. Am. Chem. Soc.* **128**, 1762–1769 (2006).
10. K. Miyatake, Y. Chikashige, E. Higuchi, M. Watanabe, Tuned polymer electrolyte membranes based on aromatic polyethers for fuel cell applications. *J. Am. Chem. Soc.* **129**, 3879–3887 (2007).
11. K. Goto, I. Rozhanskii, Y. Yamakawa, T. Otsuki, Y. Naito, Development of aromatic polymer electrolyte membrane with high conductivity and durability for fuel cell. *Polym. J.* **41**, 95–104 (2009).
12. B. Bae, T. Yoda, K. Miyatake, H. Uchida, M. Watanabe, Proton-conductive aromatic ionomers containing highly sulfonated blocks for high-temperature-operable fuel cells. *Angew. Chem. Int. Ed.* **49**, 317–320 (2010).
13. N. Li, C. Wang, S. Y. Lee, C. H. Park, Y. M. Lee, M. D. Guiver, Enhancement of proton transport by nanochannels in comb-shaped copoly(arylene ether sulfone)s. *Angew. Chem. Int. Ed.* **50**, 9158–9161 (2011).
14. K. Si, R. Wycisk, D. Dong, K. Cooper, M. Rodgers, P. Brooker, D. Slattery, M. Litt, Rigid-rod poly(phenylenesulfonic acid) proton exchange membranes with cross-linkable biphenyl groups for fuel cell applications. *Macromolecules* **46**, 422–433 (2013).
15. C. H. Fujimoto, M. A. Hickner, C. J. Cornelius, D. A. Loy, Ionomeric poly(phenylene) prepared by Diels–Alder polymerization: Synthesis and physical properties of a novel polyelectrolyte. *Macromolecules* **38**, 5010–5016 (2005).
16. T. J. G. Skalski, B. Britton, T. J. Peckham, S. Holdcroft, Structurally-defined, sulfo-phenylated, oligophenylenes and polyphenylenes. *J. Am. Chem. Soc.* **137**, 12223–12226 (2015).
17. M. Adamski, T. J. G. Skalski, B. Britton, T. J. Peckham, L. Metzler, S. Holdcroft, Highly stable, low gas crossover, proton-conducting phenylated polyphenylenes. *Angew. Chem. Int. Ed.* **56**, 9058–9061 (2017).
18. W. Zhang, E. D. Gomez, S. T. Milner, Predicting chain dimensions of semiflexible polymers from dihedral potentials. *Macromolecules* **47**, 6453–6461 (2014).
19. B. Kuei, E. D. Gomez, Chain conformations and phase behavior of conjugated polymers. *Soft Matter* **13**, 49–67 (2017).
20. D. Poppe, H. Frey, K. D. Kreuer, A. Heinzel, R. Mülhaupt, Carboxylated and sulfonated poly(arylene-*co*-arylene sulfone)s: Thermostable polyelectrolytes for fuel cell applications. *Macromolecules* **35**, 7936–7941 (2002).
21. T. Rager, M. Schuster, H. Steininger, K.-D. Kreuer, Poly(1,3-phenylene-5-phosphonic acid), a fully aromatic polyelectrolyte with high ion exchange capacity. *Adv. Mater.* **19**, 3317–3321 (2007).
22. I. Cacelli, G. Prampolini, Torsional barriers and correlations between dihedrals in *p*-polyphenyls. *J. Phys. Chem. A* **107**, 8665–8670 (2003).
23. R. A. Vaia, D. Dudis, J. Henes, Chain conformation and flexibility of thorny rod polymers. *Polymer* **39**, 6021–6036 (1998).
24. N. Yokota, M. Shimada, H. Ono, R. Akiyama, E. Nishino, K. Asazawa, J. Miyake, M. Watanabe, K. Miyatake, Aromatic copolymers containing ammonium-functionalized oligophenylene moieties as highly anion conductive membranes. *Macromolecules* **47**, 8238–8246 (2014).
25. T. Yamamoto, M. Abe, B. Wu, B.-K. Choi, Y. Harada, Y. Takahashi, K. Kawata, S. Sasaki, K. Kubota, Basic information on nonsubstituted polyphenylene and polythiophene obtained via solubilization of polymers. *Macromolecules* **40**, 5504–5512 (2007).
26. T. Mochizuki, M. Uchida, K. Miyatake, Simple, effective molecular strategy for the design of fuel cell membranes: Combination of perfluoroalkyl and sulfonated phenylene groups. *ACS Energy Lett.* **1**, 348–352 (2016).
27. J. Miyake, T. Mochizuki, K. Miyatake, Effect of the hydrophilic component in aromatic ionomers: Simple structure provides improved properties as fuel cell membranes. *ACS Macro Lett.* **4**, 750–754 (2015).
28. T. Yamamoto, B. Wu, B.-K. Choi, K. Kubota, Soluble copolymers of *p*-phenylene and *m*-phenylene. Their basic properties. *Chem. Lett.* **29**, 720–721 (2000).
29. B. Bae, T. Hoshi, K. Miyatake, M. Watanabe, Sulfonated block poly(arylene ether sulfone) membranes for fuel cell applications via oligomeric sulfonation. *Macromolecules* **44**, 3884–3892 (2011).
30. M. Inaba, T. Kinumoto, M. Kiriake, R. Umebayashi, A. Tasaka, Z. Ogumi, Gas crossover and membrane degradation in polymer electrolyte fuel cells. *Electrochim. Acta* **51**, 5746–5753 (2006).
31. T. Miyahara, T. Hayano, S. Matsuno, M. Watanabe, K. Miyatake, Sulfonated polybenzophenone/poly(arylene ether) block copolymer membranes for fuel cell applications. *ACS Appl. Mater. Interfaces* **4**, 2881–2884 (2012).
32. S. M. MacKinnon, T. J. Fuller, F. D. Coms, M. R. Schoeneweiss, C. S. Gittleman, Y.-H. Lai, R. Jiang, A. M. Brenner, Fuel cells—Proton-exchange membrane fuel cells | Membranes: Design and characterization, in *Encyclopedia of Electrochemical Power Sources* (Academic Press, 2009), pp. 741–754.
33. K. Miyatake, H. Furuya, M. Tanaka, M. Watanabe, Durability of sulfonated polyimide membrane in humidity cycling for fuel cell applications. *J. Power Sources* **204**, 74–78 (2012).
34. H. Ishikawa, Y. Fujita, J. Tsuji, M. Kusakabe, J. Miyake, Y. Sugawara, K. Miyatake, M. Uchida, Durability of sulfonated phenylene poly(arylene ether ketone) semiblock copolymer membrane in wet-dry cycling for PEFCs. *J. Electrochem. Soc.* **164**, F1204–F1210 (2017).


**Acknowledgments:** We thank T. Kimura and J. Inukai for collecting the SAXS profile at the University of Yamanashi. We also thank Y. Fujita, H. Ishikawa, and Y. Sugawara for evaluating the mechanical durability involving wet-dry cycling (DOE protocol) at Panasonic Corporation. **Funding:** This work was partly supported by the New Energy and Industrial Technology Development Organization (NEDO) through the SPer-FC Project and by the Ministry of Education, Culture, Sports, Science and Technology of Japan through a Grant-in-Aid for Young Scientists (16K18258) and Scientific Research (26289254). **Author contributions:** K.M. developed the intellectual concept, designed all the experiments, and supervised this research. J.M. constructed the novel design principle and performed the modeling work. R.A. and R.T. prepared the QP monomer and the SPP-QP copolymer, respectively. R.S., T.M., and M.U. performed the MEA fabrication and testing experiments of the fuel cells. J.M. and K.M. analyzed all experimental data and wrote the paper. **Competing interests:** The authors declare that they have no competing interests. **Data and materials availability:** All data needed to evaluate the conclusions in the paper are present in the paper and/or the Supplementary Materials. Additional data related to this paper may be requested from the authors.

Submitted 8 June 2017
Accepted 3 October 2017
Published 25 October 2017
10.1126/sciadv.aao0476

**Citation:** J. Miyake, R. Taki, T. Mochizuki, R. Shimizu, R. Akiyama, M. Uchida, K. Miyatake, Design of flexible polyphenylene proton-conducting membrane for next-generation fuel cells. *Sci. Adv.* **3**, eaao0476 (2017).

Science Advances

# Design of flexible polyphenylene proton-conducting membrane for next-generation fuel cells

Junpei Miyake, Ryunosuke Taki, Takashi Mochizuki, Ryo Shimizu, Ryo Akiyama, Makoto Uchida and Kenji Miyatake

*Sci Adv* **3** (10), eaao0476.
DOI: 10.1126/sciadv.aao0476